

# Closed-Form Specified-Fuel Commands for On–Off Thrusters

William Singhose\* and Erika Biediger†

Georgia Institute of Technology, Atlanta, Georgia 30332

Hideto Okada‡

NEC Toshiba Space Systems, Ltd., Yokohama 224-8555, Japan

and

Saburo Matunaga§

Tokyo Institute of Technology, Tokyo 152-8552, Japan

**A procedure is presented for generating on–off thruster commands for rest-to-rest slewing of flexible systems. The command profiles induce a low level of residual vibration and can be designed to use any desired amount of thruster fuel. A key advantage of the proposed method is that the commands are described by closed-form functions of the system parameters and the desired move distance. Performance measures such as maneuver speed, maximum transient deflection, and robustness to modeling errors indicate that the commands are attractive alternatives to time/fuel optimal commands that must be determined using a numerical optimization. Experimental results from a system driven by on–off air thrusters verify the proposed method.**

## I. Introduction

**M**ANY techniques have been developed for generating command profiles that eliminate residual vibration. A specific area of application for these methods is the slewing of flexible spacecraft with reaction jets. Given the on–off nature of the actuators, “smooth” commands<sup>1–4</sup> cannot be used. However, several methods have been developed to generate on–off commands that produce low levels of vibration.<sup>5–10</sup> Additional advancements have been made to increase robustness to modeling errors,<sup>5,7,9</sup> to limit the amount of transient deflection,<sup>11</sup> and to control the fuel usage.<sup>12–17</sup>

Unfortunately, most of the proposed methods require a nonlinear numerical optimization that can be difficult to implement in real time. The problems associated with optimization-based commands have motivated the development of on–off commands that can be described in closed form.<sup>18,19</sup> This paper extends this line of research by presenting a method that allows the fuel usage to be specified.

To generate commands that can be described in closed form, we assume that the command consists of three components. The first part accelerates the system, the second part is a coast period, and the third part decelerates the system back to rest. If the acceleration and deceleration portions do not cause residual vibration, then the entire command will not cause residual vibration. The proposed commands are shown in Fig. 1.

The method presented in the following section creates on–off commands that can be represented as closed-form functions of the desired move distance, fuel usage, natural frequency, and force-to-mass ratio. In Sec. III, the performance of the commands is evaluated as a function of move distance and fuel usage. In Sec. IV, the experimental results are reported, and conclusions are presented.

## II. Closed-Form Command Generation

The command generation method presented here will be demonstrated by considering the benchmark undamped two-mass and spring system.<sup>13,20</sup> Because a linear system is being considered, the technique of input shaping can be used to form the command profiles.<sup>21</sup> The phrase input shaping is used here to describe the process of convolving an input function with a sequence of impulses to produce a specially shaped command profile. Figure 2 shows that convolving a step function with a sequence of  $\pm 1$  impulses will produce a sequence of positive on–off pulses. This pulse sequence can be used to accelerate a flexible system without vibration if the impulse times are selected correctly. To create a sequence of negative pulses that decelerate the system, the signs of the impulse amplitudes are switched.

To control the amount of fuel used during a slew, the total duration of the command pulses must be limited. This requires

$$-t_1 + t_2 - t_3 + t_4 \cdots -t_{m/2-1} + t_{m/2} \leq U/2 \quad (1)$$

where  $U$  is the desired fuel usage in seconds and  $m$  is the number of command switches in the entire command profile (acceleration, coast, and deceleration). If this fuel usage constraint is combined with the traditional input shaping constraint equations that limit residual vibration, then an appropriate acceleration segment can be determined. For the acceleration pulses to cause zero residual vibration, the impulses used in the input shaping process must satisfy the following equation<sup>21</sup>:

$$0 = \sqrt{[\sum A_i \sin(\omega t_i)]^2 + [\sum A_i \cos(\omega t_i)]^2} \quad (2)$$

where  $A_i$  are the impulse amplitudes,  $t_i$  are the impulse time locations, and  $\omega$  is the natural frequency of the system's vibration. The zero vibration (ZV) equation given in Eq. (2) is derived by superimposing the response of the system to a sequence of impulses. The amplitude of this response is then extracted and set equal to zero. Details on this derivation can be found in numerous references.<sup>21,22</sup> Note that Eq. (2) produces two constraint equations because the sine and cosine summations are squared, and therefore, they both must equal zero independently. That is,

$$0 = \sum A_i \sin(\omega t_i), \quad 0 = \sum A_i \cos(\omega t_i) \quad (3)$$

Commands that satisfy Eq. (3) are called ZV commands because they force the residual vibration to zero. Commands that are very robust to modeling errors can be obtained by enforcing additional constraints.<sup>5,7,9</sup> The methods in this paper are compatible with additional robustness constraints. However, the main purpose of this

Received 30 December 2004; revision received 11 March 2005; accepted for publication 16 March 2005. Copyright © 2005 by William Singhose. Published by the American Institute of Aeronautics and Astronautics, Inc., with permission. Copies of this paper may be made for personal or internal use, on condition that the copier pay the \$10.00 per-copy fee to the Copyright Clearance Center, Inc., 222 Rosewood Drive, Danvers, MA 01923; include the code 0731-5090/06 \$10.00 in correspondence with the CCC.

\*Associate Professor, Woodruff School of Mechanical Engineering, 813 Ferst Drive; William.Singhose@me.gatech.edu.

†Research Assistant, Woodruff School of Mechanical Engineering, 813 Ferst Drive; gte377k@prism.gatech.edu.

‡Research Engineer, Space Subsystem and Equipment Division, 4035 Ikebe-cho, Tsuzuki-ku; hideoka@zg7.so-net.ne.jp.

§Associate Professor, Department of Mechanical and Aerospace Engineering, 2-12-1 O-okayama, Meguro-ku; Matunaga.Saburo@horse.mes.titech.ac.jp.

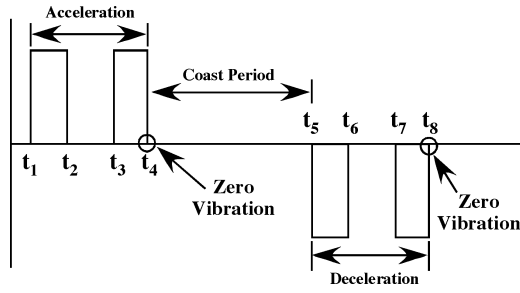


Fig. 1 Proposed on-off command profiles.

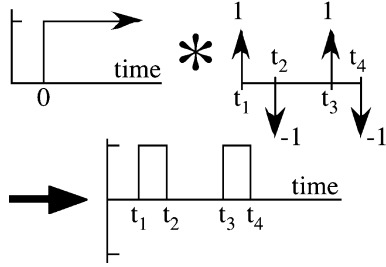


Fig. 2 Input shaping to generate a sequence of pulses.

paper is controlling fuel usage; therefore, only ZV commands will be considered.

The acceleration pulses that satisfy the ZV constraints must satisfy requirements (1) and the two constraints in Eq. (3). We seek an acceleration profile containing two pulses because the command will have three unknowns and this matches the number of constraint equations. Such a command is shown in Fig. 2, and the unknowns that must be determined are the impulse time locations,  $t_2$ ,  $t_3$ , and  $t_4$ . The time of the first impulse,  $t_1$ , is assumed to be zero. Given that we are considering an undamped system, we can assume that the command should be antisymmetric. Therefore, determining the acceleration profile also determines the deceleration profile.

There are a number of ways in which the pulses shown in Fig. 2 can produce zero residual vibration by satisfying Eq. (2). One case is when the vibration induced by the impulse at  $t_3$  cancels the vibration from the impulse at  $t_1$  and the impulse at  $t_4$  cancels the vibration caused by the impulse at  $t_2$ . Another way to cancel vibration is to have the impulse at  $t_2$  cancel the vibration from the impulse at  $t_1$  and the impulse at  $t_4$  cancel that from the impulse at  $t_3$ . Here, our main objective is finding a closed-form method of describing the command profile; therefore, we will exploit the simple case when  $t_3$  cancels  $t_1$  and  $t_4$  cancels  $t_2$ . Keeping the command duration as short as possible is also a primary objective. The following derivation accomplishes these two goals.

The amplitude of the impulse at  $t_3$  is the same as that of the first impulse. Therefore, the vibration induced by the first impulse can be canceled if  $t_3$  is located at an odd multiple of  $T/2$ , where  $T$  is the period of vibration,

$$t_3 = (2n + 1)T/2 \quad n = 0, 1, 2, \dots \quad (4)$$

The vibration induced by the impulses at  $t_2$  and  $t_4$  will also cancel if they are separated by the odd multiple chosen for  $t_3$ ,

$$t_4 - t_2 = t_3 \quad (5)$$

Given that the command contains two pulses, then the constraint of requirement (1) reduces to

$$(t_2 - t_1) + (t_4 - t_3) \leq U/2 \quad (6)$$

Enforcing the time order of the impulses requires

$$t_2 < t_3 \quad (7)$$

Solving for the possible range of fuel usage given any value of  $n$ , while minimizing  $t_4$ , yields

$$U < (4n + 2)T \quad (8)$$

By the use of inequality (8), the value of  $n$  for any desired amount of fuel usage can be obtained. Once  $n$  is known, then the impulse times that describe the acceleration pulses can be determined by using computations (4–6). These impulse times are

$$t_1 = 0, \quad t_2 = U/4, \quad t_3 = (2n + 1)T/2, \quad t_4 = t_3 + (U/4) \quad (9)$$

To summarize, Eqs. (9) describe the on-off switch times of a two-pulse command that accelerates the system without causing residual vibration, while at the same time using  $U/2$  s worth of actuator fuel. It uses  $U/2$  s of fuel because the other half of the fuel is needed to decelerate the system.

The switch times given in Eqs. (9) determine the pulses for the acceleration and by switching the impulse amplitude signs, the deceleration periods. However, the command is not complete until the duration of the coast period is determined. This duration can be calculated from the rigid-body dynamics. If a system has mass  $M$  and the position of the system's center of mass is  $x$ , then

$$\ddot{x}(t) = F(t)/M \quad (10)$$

If the system starts at rest, then the final velocity and displacement at the end of the command profile are

$$v_d = \int_0^{t_f} \frac{F(t)}{M} dt \quad (11)$$

$$x_d = \int_0^{t_f} \left[ \int_0^{t_f} \frac{F(t)}{M} dt \right] dt \quad (12)$$

For rest-to-rest motion, Eq. (11) must equal zero and Eq. (12) must equal the desired move distance. Because the forcing function  $F(t)$  is an on-off function, piecewise integration of Eqs. (11) and (12) can yield a closed-form solution. Profiles for undamped systems are particularly easy to obtain because the equations only need to be integrated up until the midpoint time  $t_m$ . For a command that contains two positive pulses and two negative pulses, the goal is to find the time at which the deceleration pulses begin. This is labeled  $t_5$  in Fig. 1. Once this time is known, then all other command switch times will be known from symmetry.

Integrating Eq. (12) up to the midpoint and setting it equal to one-half the desired slew distance yields

$$x_d/2 = \alpha/2(-t_2^2 + t_3^2 - t_4^2) + \alpha(t_2 t_m - t_3 t_m + t_4 t_m) \quad (13)$$

where  $\alpha$  is the force-to-mass ratio. The value of  $\alpha$  comes from the amplitude of the thruster force divided by the mass of the spacecraft. This is not an independently variable parameter available for modification by the controls engineer. It comes from the mechanical design of the spacecraft. Note that over time, as the thruster fuel is used, the spacecraft will lose mass and the value of  $\alpha$  will increase.

Using the symmetry of the profile, we know that the midpoint time is

$$t_m = (t_4 + t_5)/2 \quad (14)$$

Substituting Eq. (14) into Eq. (13) and solving for  $t_5$  gives

$$t_5 = \frac{x_d/\alpha + t_2^2 - t_3^2 - t_2 t_4 + t_3 t_4}{t_2 - t_3 + t_4} \quad (15)$$

The start of the deceleration is now known as a function of the desired slew distance, the force-to-mass ratio, and the switch times of the acceleration pulses, which are given in Eqs. (9). Substituting Eqs. (9) into Eq. (15), we get a very simple answer,

$$t_5 = 2x_d/(\alpha U) \quad (16)$$

The entire command is now known in closed form,

$$\begin{aligned} t_1 &= 0, & t_2 &= U/4, & t_3 &= (2n+1)T/2 \\ t_4 &= t_3 + (U/4), & t_5 &= 2x_d/(\alpha U), & t_6 &= t_5 + (t_4 - t_3) \\ t_7 &= t_5 + (t_4 - t_2), & t_8 &= t_5 + t_4 \end{aligned} \quad (17)$$

The value of  $n$  used to calculate  $t_3$  is obtained from inequality (8).

Note that if the move distance is held constant and the fuel usage is increased, then  $t_2$  will increase until it equals  $t_3$ . A further increase in fuel usage will cause  $t_3$  to jump to the next odd multiple of the half-period of system vibration. This causes a discontinuous jump in the duration of the command. Another interesting event occurs when  $t_4$  increases in value and equals  $t_5$ . After this point, additional fuel cannot be used because the desired fuel usage (measured in seconds) exceeds the maneuver time.

To demonstrate these two phenomena, Fig. 3 shows a typical example of the command switch times as a function of the fuel usage. As the fuel usage increases going from left to right, the value of  $t_2$  increases linearly. When  $t_2$  equals  $t_3$ , the value of  $n$  in Eq. (17) increases by 1 and the second pulse jumps to  $\frac{3}{2}$  of the vibration period. Note that this causes a discontinuous increase in the command duration. Figure 3 also shows the case when  $t_4$  and  $t_5$  approach each other. Choosing a large value of fuel usage, so that  $t_4$  and  $t_5$  are nearly equal, does not provide an advantage. At these high levels of fuel usage, using additional fuel provides only a marginal improvement in speed. This result indicates that high fuel usage is wasteful. In fact, most realistic cases of fuel usage would have relatively long-coast durations between the acceleration pulses and the deceleration pulses.

### III. Performance Evaluation

In this section, the performance of the proposed commands is evaluated on the benchmark undamped two-mass and spring system shown in Fig. 4. The value of the spring constant and each mass is set equal to one, as is the maximum actuator effort. This leads to a force-to-mass ratio of 0.5 and a natural frequency of  $\sqrt{2}$  rad/s.

The switch times of the command profile are fairly simple functions of the system parameters and move distance, as demonstrated by Eq. (17). However, given the variation of switch times shown in Fig. 3, it is apparent that the performance will depend on the desired fuel usage. It will also depend on the desired move distance  $x_d$ . Figure 3 shows the command switch times for the benchmark system when  $x_d = 100$  units and the fuel usage  $U$  is varied. Figure 5 shows the response of the second mass to several of these closed-form commands. In each case, the system translates to the desired location. Figure 6 shows the spring deformation. In each case, there is some transient deflection during the acceleration phase and decel-

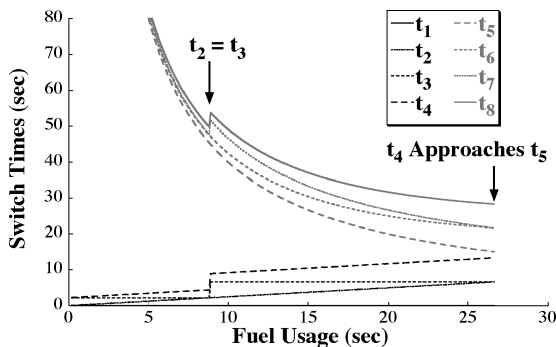


Fig. 3 Switch times as function of fuel usage.

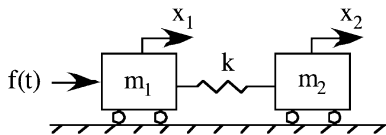


Fig. 4 Benchmark mass-spring system.

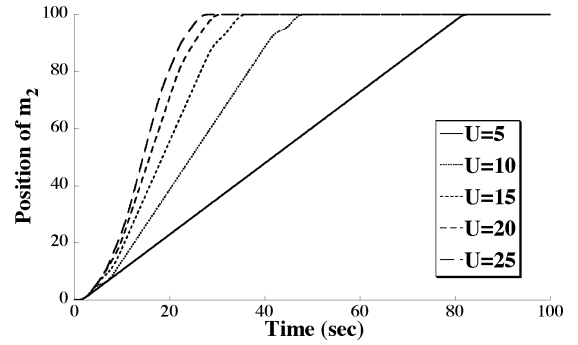


Fig. 5 Position of second mass as function of fuel usage.

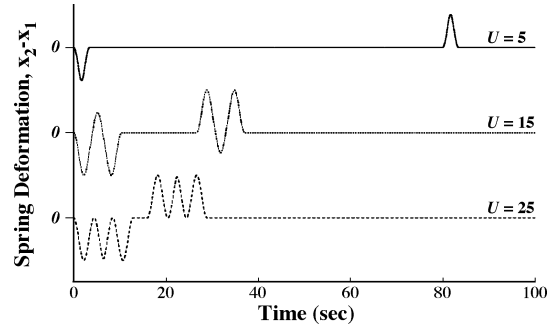


Fig. 6 Deflection as function of fuel usage.

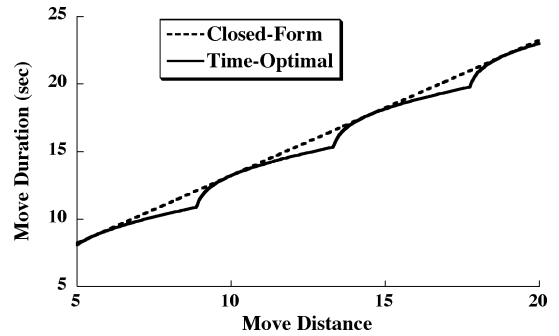


Fig. 7 Move duration as function of move distance.

eration phase. However, there is no deflection during the coasting motion, and most important, there is no residual vibration.

The performance measures discussed in this section include 1) move duration, 2) maximum transient deflection, and 3) robustness to modeling errors. First, the fuel usage was set to 4 s and the performance was determined for move distances ranging between 5 and 25 units. Then, the move distance was fixed at 5 units and the fuel usage was varied. To provide a comparison, the corresponding data were obtained for the time-optimal specified-fuel commands that are generated with a numerical optimization.<sup>15</sup> In the sequel, closed-form commands (CF) and time-optimal commands (TO) are discussed.

#### A. Dependence on Move Distance

An important aspect to consider is how long a maneuver will take. The move duration for the CF and TO commands are compared in Fig. 7 as a function of the move distance. Recall that the fuel used is fixed at 4 s. The TO commands average only 0.42 s faster than the CF commands over the range shown. Although the CF commands introduce a time penalty, it is almost negligible. This minor drawback is more than offset by the advantage of the commands being known in closed form and by the performance advantages discussed next.

The transient deflection of the system is an important measure because a large deflection induces large internal stresses. Figure 8 shows the maximum deflection as a function of move distance. The CF commands almost always cause less deflection than the TO

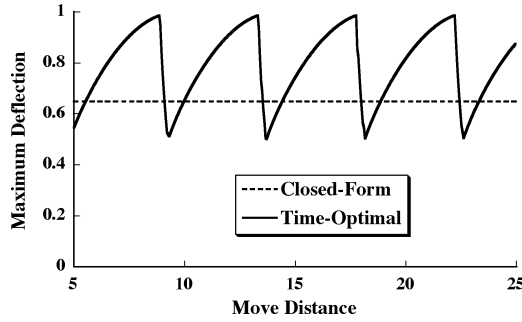


Fig. 8 Maximum deflection vs move distance.

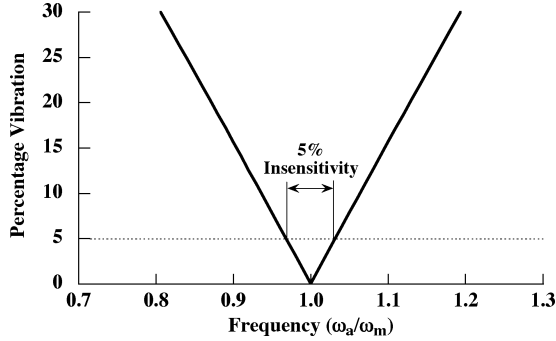


Fig. 9 Sensitivity curve.

commands. Note that the maximum deflection caused by the CF commands is constant for all values of the move distance. This is because the commands are required to have zero residual vibration after each acceleration period, meaning that the maximum deflection will occur during the acceleration period. Because the acceleration command is the same for every move distance shown, the transient deflection is the same for all move distances. On the other hand, the deflection induced by the TO commands varies in a sawtooth pattern. This effect is caused by the variation in the acceleration phase of the TO commands.

Accurate modeling of flexible systems is often difficult, and so the need for robustness to modeling errors is extremely important. When there is an error in the estimation of the system's vibration period, then some amount of residual vibration will exist. This effect is demonstrated by the sensitivity curve shown in Fig. 9. The percentage vibration shown on the vertical axis is the amount of vibration caused by the on-off command divided by the vibration induced by a single step in actuator effort. The horizontal axis is a nondimensional frequency formed by dividing the actual frequency  $\omega_a$  by the modeling frequency  $\omega_m$ . If a command can keep the vibration at a low level over a wide range of frequencies, then it would be considered robust to modeling errors.

To measure robustness quantitatively, the insensitivity is defined as the width of the sensitivity curve at a low level of vibration. In Fig. 9, the width of the curve at 5% residual vibration has been labeled as the 5% insensitivity. Figure 10 shows the 5% insensitivity to modeling errors as a function of move distance. The curves describing the insensitivity vary considerably. However, the CF commands are almost always significantly more robust than the TO commands. To obtain an average robustness measure over a range of move distances, the area under the curve can be computed. The area under the CF curve is approximately three times that of the TO curve for the range shown.

### B. Dependence on Fuel Usage

To show the effect of fuel usage, the move distance was fixed at 5 units and the fuel usage was varied. Figure 11 shows the move duration as a function of the fuel usage. As expected, the TO commands are faster for every fuel usage. However, the CF commands average less than 1 s longer than the TO commands over the range shown. Figure 12 shows a comparison of the maximum deflection caused by

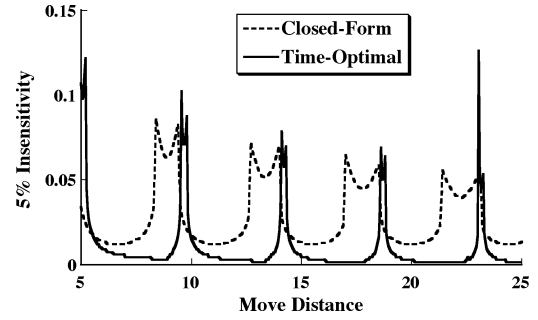


Fig. 10 Insensitivity of 5% vs move distance.

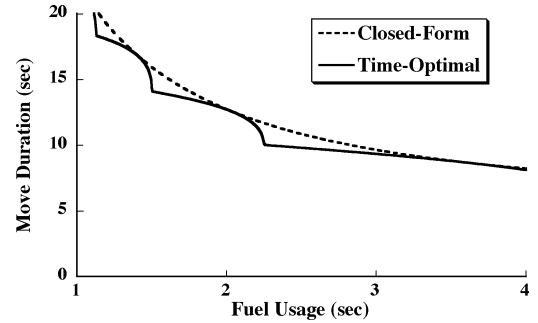


Fig. 11 Move duration vs fuel usage.

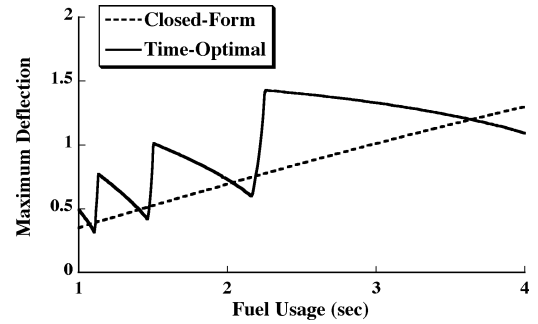


Fig. 12 Maximum deflection vs fuel usage.

the CF and TO commands as a function of the fuel usage. The data show that the maximum deflection induced by the TO commands varies considerably with fuel usage, whereas the deflection induced by the CF increases somewhat linearly. Figure 12 also shows that the maximum deflection from the TO commands is higher for most of the cases. The robustness of the shaper also varies with fuel usage. Figure 13 shows the 5% insensitivity as a function of the fuel usage. The area under the CF curve is approximately three times that of the area under the TO curve.

### C. Robustness to Thruster Firing Accuracy

Perfect cancellation of the vibration requires that the thrusters be turned on and off at the correct times. Note, however, that the thrusters do not have to transition immediately between on and off states. The thruster force could transition linearly, with a ramp function, and the vibration could still be completely canceled. This excellent feature of the commands originates from the ZV impulse sequence used to generate the commands. This input shaper can be convolved with any function and the result will still produce zero residual vibration. Therefore, the step function used in the convolution process of Fig. 2 could be replaced with a ramp function. The resulting shaped command would not be on-off in nature, but rather it would be composed of thruster bursts that transition with finite slopes. These more realistic input functions would also cause zero vibration.

If the thruster bursts are not timed perfectly, then there will be some residual vibration. This effect is very similar to the errors in

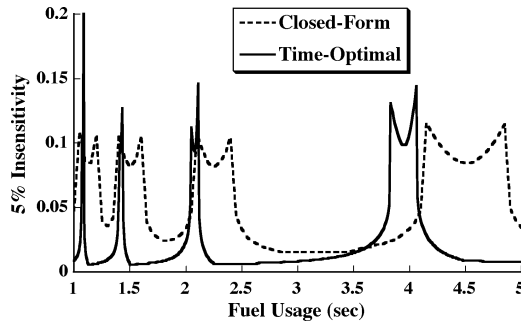


Fig. 13 Insensitivity of 5% vs fuel usage.

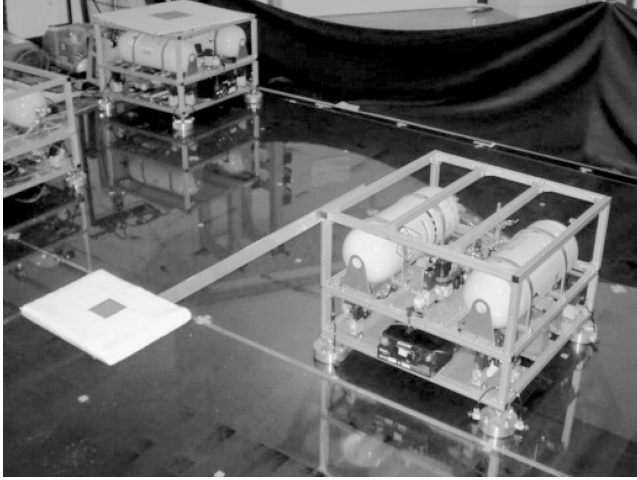


Fig. 14 Two-dimensional spacecraft dynamics simulator.

frequency shown in Fig. 9. Given that the thruster bursts will be controlled by a digital computer, their timing resolution is approximately equal to the resolution of the digital sampling rate. As long as the control loop is running approximately 10 times faster than the oscillation frequency, then the roundoff error will not be significant.<sup>23</sup> The robustness to inaccuracies in both the thruster timing and the transient response of the thruster force is best demonstrated by hardware experiments using thrusters that have both of these defects. The next section provides such a demonstration.

#### IV. Experimental Results

To test the specified-fuel commands proposed here, experiments were conducted at the Tokyo Institute of Technology. The Two-Dimensional Spacecraft Dynamics Simulator setup<sup>24</sup> is shown in Fig. 14. The facility has a  $3 \times 5$  m flat glass surface, three satellite simulators that float on the glass using air bearings, and an image processing system measuring two-dimensional position. A schematic diagram of a dynamics and intelligent control simulators for satellite clusters (DISC) unit is shown in Fig. 15.

The position and attitude ( $x, y, \theta$ ) of the DISC units are manipulated by air thrusters that are controlled by a wireless local area network (LAN). The DISC units are equipped with eight thrusters, two on each side, as shown in Fig. 15. By the firing of the thrusters in various combinations, the three-dimensional positioning can be controlled. The air thrusters use regulated pressure up to 500 psi (3.45 MPa). However, the experiments conducted for this work used 100 psi (0.7 MPa). The system mimics many of the important dynamic effects in on-off thruster control of satellites. For example, on-off thrusters never produce a perfect pulse in force; there is always a transient rise and fall in the thrust force. Furthermore, the thrust force is never perfectly constant when it reaches its peak value. These effects are readily apparent in the air thruster system used to move the DISC units. Another realistic inconvenience is the time delays in the command sequence due to using the LAN to issue thruster commands.

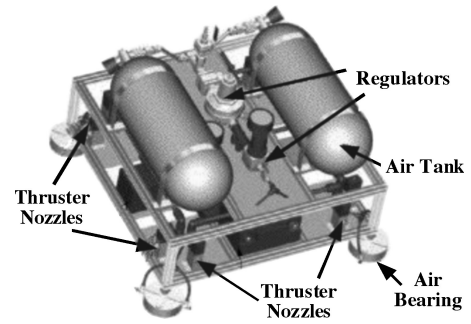


Fig. 15 Schematic diagram of DISC unit.

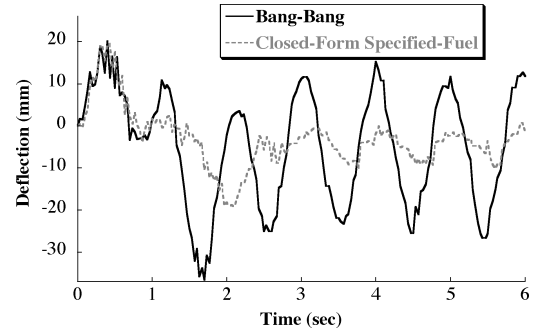


Fig. 16 Deflection and residual vibration for a 45-deg rotation.

To test the commands developed here, a flexible appendage with an endpoint tracking target was attached to a DISC unit, as shown in Fig. 14. Both the length and endpoint mass of the flexible beam were adjustable. Numerous experiments were conducted to evaluate various on-off thruster commands for a variety of move distances and appendage dynamics. In each case, a DISC unit was initially allowed to float freely on the air bearings. Then, a sequence of thruster firings was performed. The overhead camera recorded the location of the main unit, as well as the endpoint of the flexible appendage.

The nominal length of the adjustable appendage was set to give a very lightly damped natural frequency of 1.0 Hz. The control system calculated on-off thruster firings for these baseline dynamics. For example, the endpoint deflection of the appendage resulting from a 45-deg rotational motion is shown in Fig. 16. As seen in Fig. 16, a bang-bang command induces both large transient deflection and residual vibration. The bang-bang command used 2.4 s of air thrust to perform the slew. Equations (17) were used to generate a command to provide the same rotation, but decrease the vibration and use only 1.8 s of air thrust. This command is described by

$$\begin{bmatrix} A_i \\ t_i \end{bmatrix} = \begin{bmatrix} 1 & -1 & 1 & -1 & -1 & 1 & -1 & 1 \\ 0 & 0.45 & 0.5 & 0.95 & 1.667 & 2.117 & 2.167 & 2.617 \end{bmatrix} \quad (18)$$

Figure 16 shows that the closed-form command reduces the residual vibration by more than 75%. The vibration is not completely eliminated due to modeling errors and nonlinearities in the system, such as the air thrusters. Note that, although the CF command uses 25% less actuator fuel, the move takes only about 9% longer. This reinforces the results shown in Figs. 7 and 11 that indicate the CF commands are very close to time optimal.

The results shown in Fig. 16 are representative of the performance over a wide range of conditions. For example, Fig. 17 shows the deflection and residual vibration induced by the CF commands as a function of fuel usage. As the fuel usage is decreased from 1.6 to 1.0 s, the maneuver takes somewhat longer to complete, as predicted by Figs. 3 and 11. This effect is indicated in Fig. 17 by the bursts of large negative deflection that occur when the system is decelerated. These bursts occur at about 2.3 s for  $U = 1.6$  and increase to 3.3 s for  $U = 1.0$ . The maximum transient deflection decreases slightly with

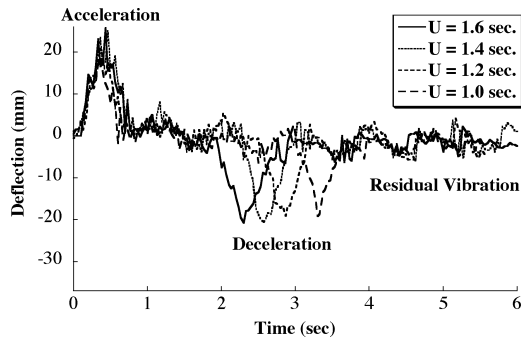


Fig. 17 Appendage deflection as function of fuel usage.

decreasing fuel usage, as predicted by Fig. 12. The residual vibration remains roughly constant as the fuel usage changes. Note that the vibration caused by the CF commands is always substantially less than the vibration induced by the unshaped bang-bang command shown in Fig. 16.

Although the experimental response is dominated by the lightly damped mode at 1.0 Hz, higher modes are readily apparent. This multimode nature of the system is a further complication that mimics actual spacecraft. However, given the dominance of the low mode, the commands were only designed to suppress the low frequency. If the higher modes were a significant problem, then the commands could be designed to suppress the higher modes as well.<sup>25</sup>

## V. Conclusions

A method for generating on-off commands that can be described in closed form was presented. The commands were designed to accelerate and decelerate a flexible system without residual vibration, while using a specified amount of actuator fuel. Although the CF commands are not equivalent to the TO commands, they are near time optimal in most cases. Furthermore, the CF commands are more robust to modeling errors and cause less transient deflection during the motion. The most significant advantage provided by the new commands is that they are described in closed form and do not need to be numerically optimized for every possible move distance and/or fuel usage. Experimental results on a system driven by air thrusters verified many of the key theoretical results.

## References

- <sup>1</sup>Farrenkopf, R. L., "Optimal Open-Loop Maneuver Profiles for Flexible Spacecraft," *Journal of Guidance and Control*, Vol. 2, No. 6, 1979, pp. 491–498.
- <sup>2</sup>Swigert, C. J., "Shaped Torque Techniques," *Journal of Guidance and Control*, Vol. 3, No. 5, 1980, pp. 460–467.
- <sup>3</sup>Thompson, R. C., Junkins, J. L., and Vadali, S. R., "Near-Minimum Time Open-Loop Slewing of Flexible Vehicles," *Journal of Guidance, Control, and Dynamics*, Vol. 12, No. 1, 1989, pp. 82–88.
- <sup>4</sup>Turner, J. D., and Junkins, J. L., "Optimal Large-Angle Single-Axis Rotational Maneuvers of Flexible Spacecraft," *Journal of Guidance and Control*, Vol. 3, No. 6, 1980, pp. 578–585.
- <sup>5</sup>Liu, Q., and Wie, B., "Robust Time-Optimal Control of Uncertain Flexible Spacecraft," *Journal of Guidance, Control, and Dynamics*, Vol. 15, No. 3, 1992, pp. 597–604.
- <sup>6</sup>Pao, L. Y., "Minimum-Time Control Characteristics of Flexible Structures," *Journal of Guidance, Control, and Dynamics*, Vol. 19, No. 1, 1996, pp. 123–129.
- <sup>7</sup>Singh, T., and Vadali, S. R., "Robust Time-Optimal Control: A Frequency Domain Approach," *Journal of Guidance, Control, and Dynamics*, Vol. 17, No. 2, 1994, pp. 346–353.
- <sup>8</sup>Tuttle, T., and Seering, W., "Creating Time Optimal Commands with Practical Constraints," *Journal of Guidance, Control, and Dynamics*, Vol. 22, No. 2, 1999, pp. 241–250.
- <sup>9</sup>Singhose, W., Derezinski, S., and Singer, N., "Extra-Insensitive Input Shapers for Controlling Flexible Spacecraft," *Journal of Guidance, Control, and Dynamics*, Vol. 19, No. 2, 1996, pp. 385–391.
- <sup>10</sup>VanderVelde, W., and He, J., "Design of Space Structure Control Systems Using On-Off Thrusters," *Journal of Guidance, Control, and Dynamics*, Vol. 6, No. 1, 1983, pp. 53–60.
- <sup>11</sup>Singhose, W., Banerjee, A., and Seering, W., "Slewing Flexible Spacecraft with Deflection-Limiting Input Shaping," *Journal of Guidance, Control, and Dynamics*, Vol. 20, No. 2, 1997, pp. 291–298.
- <sup>12</sup>Meyer, J. L., and Silverberg, L., "Fuel Optimal Propulsive Maneuver of an Experimental Structure Exhibiting Spacelike Dynamics," *Journal of Guidance, Control, and Dynamics*, Vol. 19, No. 1, 1996, pp. 141–149.
- <sup>13</sup>Singh, T., "Fuel/Time Optimal Control of the Benchmark Problem," *Journal of Guidance, Control, and Dynamics*, Vol. 18, No. 6, 1995, pp. 1225–1231.
- <sup>14</sup>Singhose, W., Bohlke, K., and Seering, W., "Fuel-Efficient Pulse Command Profiles for Flexible Spacecraft," *Journal of Guidance, Control, and Dynamics*, Vol. 19, No. 4, 1996, pp. 954–960.
- <sup>15</sup>Singhose, W., Singh, T., and Seering, W., "On-Off Control with Specified Fuel Usage," *Journal of Dynamic Systems, Measurement, and Control*, Vol. 121, No. 2, 1999, pp. 206–212.
- <sup>16</sup>Souza, M. L. O., "Exactly Solving the Weighted Time/Fuel Optimal Control of an Undamped Harmonic Oscillator," *Journal of Guidance, Control, and Dynamics*, Vol. 11, No. 6, 1988, pp. 488–494.
- <sup>17</sup>Wie, B., Sinha, R., Sunkel, J., and Cox, K., "Robust Fuel- and Time-Optimal Control of Uncertain Flexible Space Structures," *Proceedings of Guidance, Navigation, and Control Conference*, AIAA, Washington, DC, 1993, pp. 939–948.
- <sup>18</sup>Singhose, W., Mills, B., and Seering, W., "Closed-Form Methods for Generating On-Off Commands for Undamped Flexible Structures," *Journal of Guidance, Control, and Dynamics*, Vol. 22, No. 2, 1999, pp. 378–382.
- <sup>19</sup>Singhose, W., Biediger, E., Okada, H., and Matunaga, S., "Control of Flexible Satellites Using Analytic On-Off Thruster Commands," AIAA Paper 2003-5333, 2003.
- <sup>20</sup>Wie, B., and Bernstein, D. S., "Benchmark Problems for Robust Control Design," *Journal of Guidance, Control, and Dynamics*, Vol. 15, No. 5, 1992, pp. 1057–1059.
- <sup>21</sup>Singer, N. C., and Seering, W. P., "Preshaping Command Inputs to Reduce System Vibration," *Journal of Dynamic Systems, Measurement and Control*, Vol. 112, March 1990, pp. 76–82.
- <sup>22</sup>Grosser, K., and Singhose, W., "Command Generation for Reducing Perceived Lag in Flexible Telerobotic Arms," *Japan Society of Mechanical Engineers International Journal*, Vol. 43, No. 3, 2000, pp. 755–761.
- <sup>23</sup>Kozak, K., and Singhose, W., "Rapid Computation of Digital Input Shaping Filters for Reconfigurable Machines," *Proceedings of Japan-USA Symposium on Flexible Automation*, JUSFA 02/U-057, American Society of Mechanical Engineers, New York, 2002.
- <sup>24</sup>Matunaga, S., Mori, O., Tsurumi, S., and Okada, H., "Robot Cluster System and its Ground Experiment System," *Proceedings of 51st Congress of the International Astronautical Federation*, Vol. IAF-00-A.3.06, International Astronautical Federation, Paris, 2000.
- <sup>25</sup>Singhose, W. E., Mills, B. W., and Seering, W. P., "Closed-Form Methods for On-Off Control of Multi-Mode Flexible Structures," *Proceedings of IEEE Conference on Decision and Control*, Vol. 2, Institute of Electrical and Electronics Engineers, Los Alamitos, CA, 1997, pp. 1381–1386.